SAND81-8201
Unlimited Release

A Simple Theory for Predicting the Natural Convective Energy Loss From Side-Facing Solar Cavity Receivers

M. Abrams, R. Greif

Prepared by Sandia Laboratories, Albuquerque, New Mexico 87115 and Livermore, California 94550 for the United States Department of Energy under Contract DE-AC04-76DP00789.

Printed January 1981

Sandia Laboratories
energy report

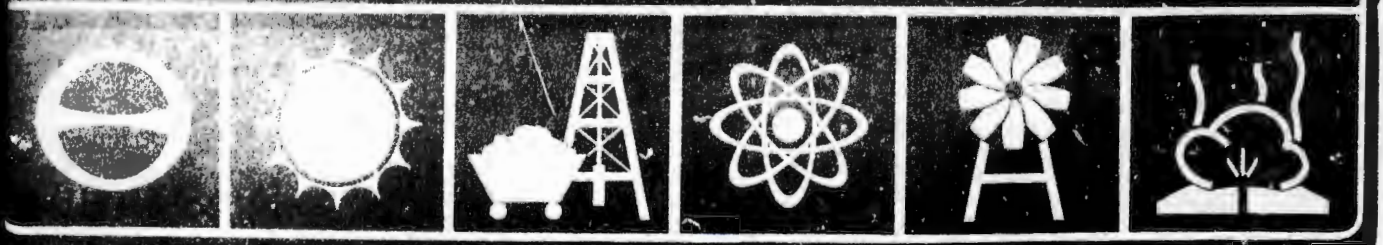

SF 2900 QQB(3 74)

Issued by Sandia National Laboratories, operated for the United States Department of Energy by Sandia Corporation.

NOTICE

SAND81-8201
Unlimited Release
Printed January 1981

A SIMPLE THEORY FOR PREDICTING THE NATURAL CONVECTIVE ENERGY LOSS FROM SIDE-FACING SOLAR CAVITY RECEIVERS

M. Abrams
Thermal Sciences Division
Sandia National Laboratories, Livermore

and

R. Greif
College of Engineering
University of California, Berkeley
Berkeley, California 94720

ABSTRACT

A simple theory for predicting the convective energy loss from side-facing cavity receivers in windless environments has been developed. The approach used is to determine the velocity distribution of the incoming air in the aperture plane (and thereby the rate of mass entrainment); and then to estimate the bulk temperature of the heated emerging air. The convective loss is then calculated from an energy balance. To illustrate this theory, numerical results applicable to the 2.15 meter cubic cavity being tested in our laboratory are provided.

CONTENTS

FOREWORD

In April 1979, at a workshop held in Dublin, California, a cross section of the nation's experts in the thermal sciences found that the extreme environment and large sizes of typical solar central receivers place them in a flow and heat transfer regime where data and proven predictive methods for estimating energy losses are lacking. Confronted with this appraisal and the urgent need to predict the efficiency and hence the cost of energy collection, the Central Receiver Energy Loss Program was initiated.

The goal of the program is the development of computational tools, to be verified by experiment, to predict the convective and radiative energy losses from external and cavity-type central receivers.

This report describes one of these tools: an approximate analytical solution for the convective energy loss from a side-facing solar cavity in a windless environment. The objectives of this work are to provide preliminary results while detailed numerical simulations of the convective process are being developed, and then afterwards, to serve as a rapid means of estimating the convective loss in applications where the more accurate numerical predictions are not needed.

NOMENCLATURE

A_s	internal surface area of cavity
a	constant defined by Equation (46)
C_c	contraction coefficient
c_p	specific heat
F	function defined by Equation (33)
f	fraction y_n/L_{ap}
g	acceleration due to gravity
h	heat transfer coefficient
k	thermal conductivity
L_{ap}	height of aperture
$\dot{m}$	rate of mass entrainment per unit width of cavity aperture
Nu	Nusselt number
Pr	Prandtl number
p	pressure
Q	rate of convective energy loss per unit width of cavity aperture
R	ideal gas constant
T	temperature (degrees absolute)
y	distance beneath neutral elevation
U	maximum velocity of emerging air
u	velocity of emerging air
V_{ap}	characteristic aperture inflow velocity

v	velocity of incoming air
W_{ap}	width of aperture

Greek:

β	coefficient of volumetric expansion
η	dimensionless distance, y/y_n (see Figure 1)
η_D	dimensionless distance, y_D/y_n (see Figure 2)
λ	dummy variable, ξ/ξ_n
ν	kinematic viscosity
ξ	distance above neutral elevation
ρ	density

Superscripts:

*	dimensionless quantity
'	dummy variable

Subscripts:

a	refers to conditions in exterior ambient plane
ap	refers to conditions in aperture plane
b	bulk
D	profile development distance
f	evaluated at film temperature
fp	flat plate
i	refers to conditions in vertical stagnant fluid column alongside vena contracta
j	refers to conditions in vena contracta
max	upper bound
min	lower bound
n	neutral elevation

T	refers to distance over which temperature profile develops
V	refers to distance over which velocity profile develops
w	wall condition

A SIMPLE THEORY FOR PREDICTING THE NATURAL CONVECTIVE ENERGY LOSS FROM SIDE-FACING SOLAR CAVITY RECEIVERS

Introduction

The present approach is closely related to that used with some success in the building sciences to predict the rate of air flow and heat transfer through doorways and corridors [e.g., 1,2,3]. In this approach, Bernoulli's equation is applied to streamlines which pass from a region where velocities are assumed to be negligible through the doorway or corridor where knowledge of the velocity distribution is sought.

In using this approach to evaluate the convective energy loss from a cavity-type receiver (Figure 1), the method is to determine the velocity distribution of the incoming air in the aperture plane (and from this the rate of mass entrainment, $\dot{m}$); and then to estimate the bulk temperature of the heated emerging air, T_b. The convective loss is then calculated from the energy balance

$$Q = \dot{m}\, c_p\, (T_b - T_a) \tag{1}$$

where T_a is the ambient temperature.

We give here expressions describing the aperture-plane velocity distribution, the rate of mass entrainment, and the bulk temperature of the heated emerging air for side-facing solar cavities in windless environments. Expressions for bounds within which entrained mass flows and convective energy losses must lie are also presented. Such bounds can serve as screening tests

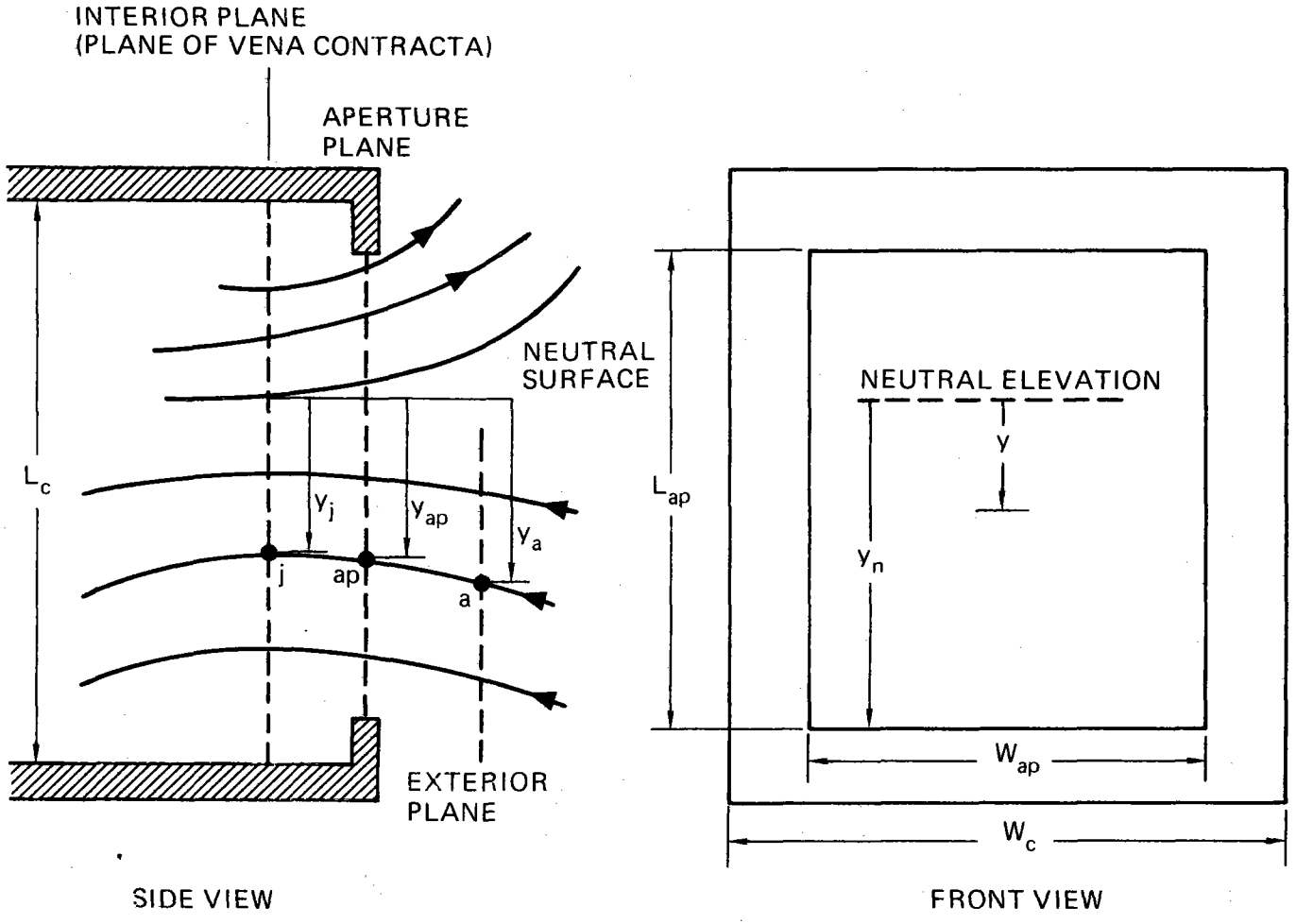

Figure 1. Flow Patterns in the Entrance Region of a Side-Facing Cavity

for this and other predictive theories. As an illustration of the present theory, numerical results applicable to the 2.15 meter cubic cavity being tested at Sandia National Laboratories are provided.

It should be noted at the outset, that the convective loss from a cavity can be determined ultimately only by direct measurement or by a detailed three-dimensional computer simulation. Any other approach, including the present one, must necessarily entail a number of assumptions and approximations. Presently, measurement and numerical techniques applicable to large turbulent cavities are being developed, and probably will be unavailable for some time. The role envisaged for the present work, therefore, is to provide tentative results in the interim, and then afterwards, to serve as a tool for making rapid estimates of the convective energy loss in applications where the more accurate computer simulations are not required.

To our knowledge, there are no published works dealing with the turbulent flow and heat transfer regimes typical of large-scale solar receivers. The only studies relevant to the problem of concern here are the numerical simulations of Penot [4,5], Eyler [6], and Humphrey, et al. [7], which are, however, limited to two dimensions and laminar flow*, and the investigations of Quintiere and Den Braven [3], and Steckler et al. [8], which are concerned with fire-induced flows through doorways. The aperture-plane velocity distributions found in these studies possess the qualitative features depicted in Figure 2a. The velocity of the incoming air increases rapidly from zero to a value V_{ap} in the velocity development region 0 to y_V, and then remains essentially constant until a narrow boundary layer region at the lower edge of the cavity

*The numerical simulations in [4-6] also use the Boussinesq approximation which is inappropriate in solar cavities where large variations in temperature can exist within the enclosed body of air. Eyler's computational procedure [6] is capable of handling three dimensions, but only two-dimensional results were presented.

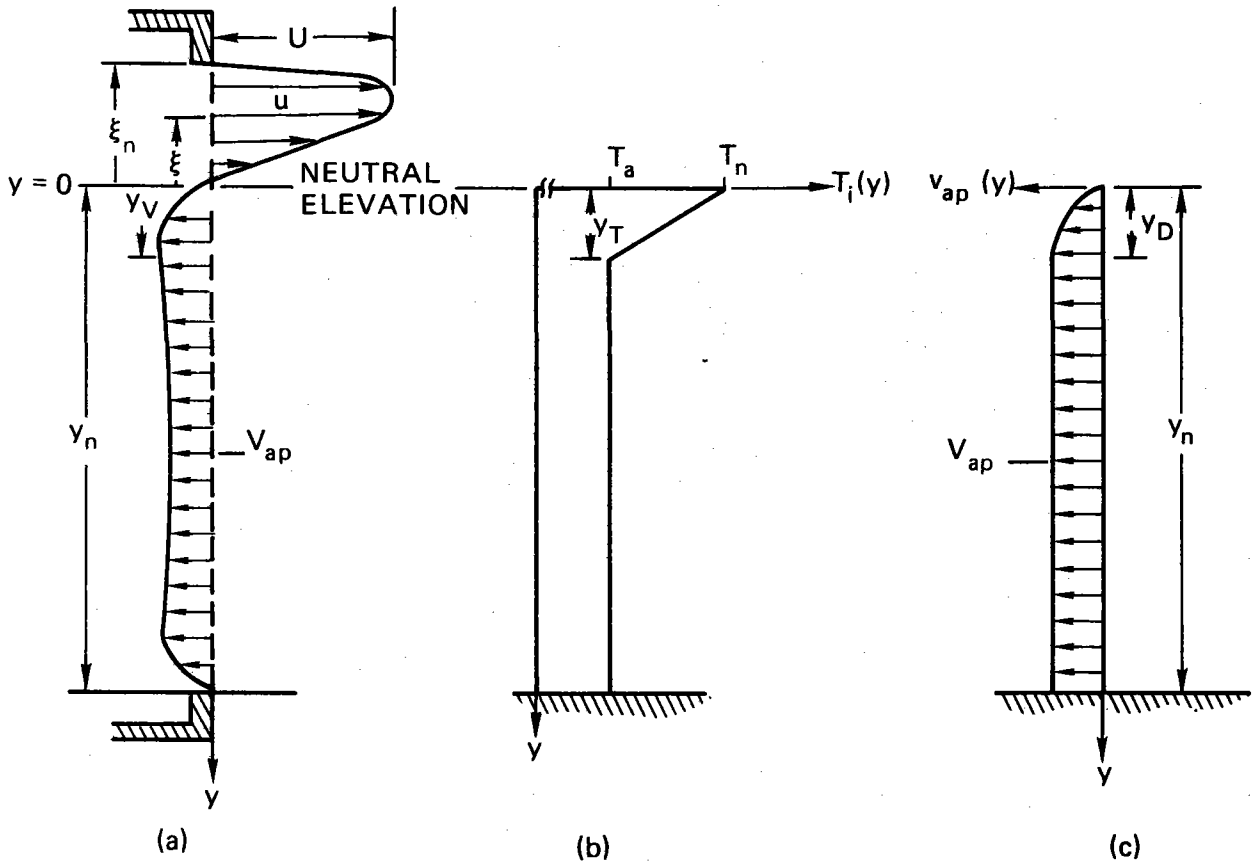

Figure 2. (a) Qualitative Features of the Aperture-Plane Velocity Distribution [3-8]

(b) Temperature Distribution in the Vertical Stagment Fluid Column Alongside the Vena Contracta (an Idealization of the Measurements Given in Reference 3)

(c) Ideal Velocity Distribution of the Incoming Air Corresponding to the Temperature Distribution Depicted in (b)

aperture. The heated emerging air possesses a velocity maximum whose location appears to shift upward as the Grashof number increases. One of the underlying assumptions in this study is that the aperture-plane velocity distribution at the center of a turbulent three-dimensional solar cavity is similar, qualitatively, to those found in References 3-8.

Analysis

1. The Velocity Distribution of the Incoming Air and the Rate of Mass Entrainment

To determine the velocity distribution of the incoming air, we consider three hypothetical, plane parallel surfaces: the aperture plane; an exterior plane sufficiently far from the cavity such that incoming air velocities may be neglected; and an interior plane located at the vena contracta of the incoming air (Figure 1). The vena contracta, or jet of minimum cross-sectional area, is bordered on all sides by a frame of essentially stagnant air. The neutral surface demarcates the inflow from the outflow region, and the air velocity is zero on this surface. The line of intersection of the neutral surface and the vena contracta plane is called the neutral elevation.

Bernoulli's equation, $gy + v^2/2 + \int dp/\rho$ = constant along a given streamline, is applied to streamlines of incoming air between the exterior and interior planes. This relationship expresses the conservation of momentum principle when viscous forces are negligible. Strictly speaking, the use of the Bernoulli equation is not valid in the velocity development region $0\text{-}y_v$ and at the lower edge of the cavity aperture (Figure 2a) where viscous forces must predominate. We shall show later, however, that since these regions are small, only negligible error results in the calculation of the rate of mass

entrainment. For concreteness, we apply Bernoulli's equation to the particular streamline which passes through points a in the exterior plane, ap in the aperture plane, and j in the vena contracta. These points are located, respectively, at distances y_a, y_{ap}, and y_j beneath the neutral elevation (see Figure 1). The result is

$$\int_a^j \frac{dp}{\rho} + \frac{v_j^2(y_j)}{2} + g\,(y_j - y_a) = 0 \qquad (2)$$

Although our concern ultimately is with the aperture plane, we deal first with the vena contracta because there streamlines have zero curvature (in horizontal planes), and hence, every streamline at the elevation y_j is at the same pressure. It is for this reason that Equation (2) is applied to all streamlines passing through the vena contracta at the elevation y_j. The transference of the velocities to the aperture plane is described subsequently.

Two additional assumptions are now made. First, it is assumed that heat transfer to the air flowing from outside the cavity to the vena contracta is negligible, and thus, the air temperature in this region is everywhere equal to T_a. Second, it is assumed that elevation differences, such as y_j-y_a, along an incoming streamline are sufficiently small so that the gravitational contribution in Equation (2) may be dropped. The first assumption and the ideal gas law, $\rho = p/RT$, lead to the result

$$\int_a^j \frac{dp}{\rho} \doteq - \frac{[p_a(y_a) - p_j(y_j)]}{\rho_a(y_a)} \qquad (3)$$

The second assumption is more difficult to justify and it may, in fact, be invalid.* It is employed here, however, because as stated earlier,

*For example, if velocities of the order of 1 m/sec are expected in the vena contracta, the gravitational contribution is 10% of the kinetic energy contribution for elevation differences $|y_j - y_a|$ on the order of ~ 0.5 cm.

it has been used by others in analyzing related phenomena. (It also greatly simplifies the analysis.)

With the neglect of the gravitational term, the combination of Equations (2) and (3) gives the following expression for the velocity distribution in the vena contracta:

$$v_j(y_j) = \sqrt{2[p_a(y_a) - p_j(y_j)]/\rho_a(y_a)} \qquad (4)^*$$

or, simply

$$v_j(y) = \sqrt{2[p_a(y) - p_j(y)]/\rho_a(y)} \qquad (5)$$

where it is assumed that

$$y_a = y_j \equiv y \; . \qquad (6)$$

The distribution of pressure in the exterior plane is taken to be hydrostatic so that

$$p_a(y) = p_n + g \int_0^y \rho_a(y')dy' \qquad (7)$$

where p_n is the pressure at the neutral elevation (Figure 1). Also, since the pressure at the elevation y in the vena contracta must equal the hydrostatic pressure at the elevation y in the stagnant vertical column of fluid alongside the vena contracta,

$$p_j(y) = p_n + g \int_0^y \rho_i(y')dy' \qquad (8)$$

where $\rho_i(y')$ represents the density distribution in that fluid column. The substitution of Equations (7) and (8) into (5) thus gives the velocity distribution in the vena contracta:

*It should be noted that the pressure difference p_a-p_j which drives the flow into the cavity is also extremely small. For instance, a velocity of 1m/sec in the vena contracta would be produced by a pressure difference of only ~ 0.06 mm water as can be calculated from Equation (4).

$$v_j(y) = \sqrt{\frac{2g\left[\int_0^y [\rho_a(y') - \rho_i(y')]dy'\right]}{\rho_a(y)}} \tag{9}$$

The determination of the velocity distribution in the aperture plane is now considered. It is customary to relate the areas of a vena contracta A_{vc} and an aperture inflow A_{ap} by a contraction coefficient C_c according to [9].

$$A_{vc} = C_c A_{ap} \tag{10}$$

Here, we assume further, that the contraction coefficient is the same for each stream tube between the aperture and the vena contracta. Thus, from the conservation of mass principle, the velocity at the aperture on any streamline, a - ap - j for example, may be expressed as

$$v_{ap}(y_{ap}) = C_c \rho_j(y_j) v_j(y_j)/\rho_{ap}(y_{ap})$$

or, simply,

$$v_{ap}(y) \triangleq C_c v_j(y), \tag{11}$$

which is a consequence of the two simplifying assumptions made earlier. For completeness, we point out that the assumption of negligible elevation differences along incoming streamlines in the Bernoulli equation may also be strictly inconsistent with the existence of a flow area contraction. The combination of Equations (9), (11) and the relationship

$$\rho_a(y') - \rho_i(y') = \frac{p}{R}\left[\frac{1}{T_a} - \frac{1}{T_i(y')}\right] \tag{12}$$

yields the velocity distribution in the aperture plane

$$v_{ap}(y) = C_c \sqrt{2g} \sqrt{\int_0^y \left[1 - \frac{T_a}{T_i(y')}\right] dy'} \tag{13}$$

It should be noted that $T_i(y')$ represents the temperature at the elevation y' in the stagnant column of fluid alongside the vena contracta; and it should be recognized that, because of the assumptions made, the contraction coefficient C_c may be more appropriately considered to be a correlation factor.

The rate of mass flow into the cavity per unit width of its aperture is given by

$$\dot{m} = \int_0^{y_n} \rho_{ap}(y)\, v_{ap}(y)\, dy \tag{14}$$

or

$$\dot{m} = \rho_a \int_0^{y_n} v_{ap}(y)\, dy \tag{15}$$

considering that, for the purpose of this integration, $\rho_{ap}(y) \approx \rho_a$. The substitution of Equation (13) into (15) then yields the rate of mass entrainment

$$\dot{m} = \rho_a\, C_c\, \sqrt{2g} \int_0^{y_n} \sqrt{\int_0^{y} \left[1 - \frac{T_a}{T_i(y')}\right] dy'}\; dy \tag{16}$$

Equations (13) and (16) may be made dimensionless by the substitution of the variables

$$\eta = y/y_n \; ; \quad \eta' = y'/y_n \; ; \quad f = y_n/L_{ap} \; ; \text{ and } T_i^* = T_i/T_a \tag{17}$$

with the results

$$v^*(\eta) \equiv \frac{v_{ap}(\eta)}{C_c\sqrt{fL_{ap}}\,\sqrt{2g}} = \sqrt{\int_0^{\eta} \left[1 - \frac{1}{T_i^*(\eta')}\right] d\eta'} \tag{18}$$

and

$$\dot{m}^* \equiv \frac{\dot{m}}{\rho_a C_c (fL_{ap})^{3/2}\,\sqrt{2g}} = \int_0^1 v^*(\eta)\, d\eta \tag{19a}$$

$$= \int_0^1 \sqrt{\int_0^{\eta} \left[1 - \frac{1}{T_i^*(\eta')}\right] d\eta'}\; d\eta \tag{19b}*$$

*Knowledge of the distance fL_{ap} $(=y_n)$ which appears in the calculation of the velocity distribution from Equation (18) is actually not required. Rather, in this equation fL_{ap} is merely the length used to normalize distance. If a length other than fL_{ap} had been used, it would appear in Equation (18) instead. The distance $fL_{ap}(=y_n)$ must be known, however, in the calculation of the rate of mass entrainment (Equations (16) or (19b)).

It is seen that, to use the building sciences approach to calculate the rate of mass entrainment, one must have a priori estimations of the aperture height occupied by the inflow, $fL_{ap}(=y_n)$; the contraction coefficient, C_c; and the function T_i (y) (or $T_i^*(\eta)$) describing the temperature distribution in the stagnant fluid column alongside the vena contracta. We now discuss the specification of this distribution.

The Temperature Distribution Function $T_i(y)$

Our specification of the temperature distribution in the stagnant fluid column alongside the vena contracta is based on the temperature measurements of Quintiere and Den Braven [3] and the requirement that the resultant incoming velocity distribution, expressed by Equation (13), must also agree qualitatively with that depicted in Figure 2a. Quintiere and Den Braven found that the temperature alongside the vena contracta of the incoming air decreased from a relatively high value, T_n, at the neutral elevation to nearly the ambient temperature, T_a, within a short distance y_T beneath the neutral elevation. An idealization of their measurements is shown in Figure 2b. The aperture plane velocity data in the Quintiere-Den Braven study indicate, further, that the region (0-y_V) within which the velocity develops from 0 to V_{ap} is approximately equal to the span (0-y_T) within which the temperature $T_i(y)$ decreases from T_n to T_a; i.e.,

$$y_V \approx y_T \equiv y_D \tag{20}$$

where y_D is considered to be the development distance for both the velocity and temperature profiles. Our specification of the temperature distribution in the fluid column alongside the vena contracta is thus assumed to be

$$T_i(y) = T_n - \frac{y}{y_D}(T_n - T_a) \text{ for } 0 < y < y_D \tag{21a}$$

and

$$T_i(y) = T_a \text{ for } y_D < y < y_n \tag{21b}$$

which in dimensionless form is:

$$T_i^*(\eta) = T_n^* - \frac{\eta}{\eta_D}(T_n^* - 1) \text{ for } 0 < \eta < \eta_D \tag{22a}$$

and

$$T_i^*(\eta) = 1 \text{ for } \eta_D < \eta < 1 \tag{22b}$$

where $$\eta_D = y_D/y_n \tag{22c}$$

Having specified the temperature distribution function $T_i(y)$, the resulting velocity distribution of the incoming air (obtained by substituting Equations (21) into (13)) is given by

$$v_{ap}(y) = C_c\sqrt{2gy_D}\sqrt{\frac{y}{y_D} + \frac{1}{T_n/T_a - 1}\ln\left[1 - \frac{y}{y_D}\left(1 - \frac{T_a}{T_n}\right)\right]} \text{ for } 0 < y < y_D \tag{23a}$$

and

$$v_{ap}(y) = C_c\sqrt{2gy_D}\sqrt{1 + \frac{1}{T_n/T_a - 1}\ln\frac{T_a}{T_n}} = \text{const} \text{ for } y > y_D \tag{23b}$$

$$\equiv V_{ap}$$

and the rate of mass entrainment (obtained by substituting Equations (23) into (15)) by

$$\dot{m} = \rho_a C_c \sqrt{2gy_D} \int_0^{y_D} \sqrt{\frac{y}{y_D} + \frac{1}{T_n/T_a - 1} \ln\left[1 - \frac{y}{y_D}\left(1 - \frac{T_a}{T_n}\right)\right]}\, dy$$

$$+ \rho_a C_c (y_n - y_D) \sqrt{2gy_D} \sqrt{1 + \frac{1}{T_n/T_a - 1} \ln \frac{T_a}{T_n}} \qquad (24)$$

It is observed that the velocity distribution (Equations (23)), which is also drawn in Figure 2c, possesses the required qualitative features shown in Figure 2a. In dimensionless form these equations are, respectively,

$$v^*(\eta) \equiv \frac{v_{ap}(\eta)}{C_c\sqrt{2g}\sqrt{fL_{ap}}} = \sqrt{\eta + \frac{\eta_D}{T_n^* - 1} \ln\left[1 - \frac{\eta}{\eta_D}\left(1 - \frac{1}{T_n^*}\right)\right]} \quad \text{for } 0<\eta<\eta_D . \qquad (25a)$$

$$v^*(\eta) \equiv \frac{v_{ap}(\eta)}{C_c\sqrt{2g}\sqrt{fL_{ap}}} = \sqrt{\eta_D}\sqrt{1 - \frac{\ln T_n^*}{T_n^* - 1}} \quad \text{for } \eta_D<\eta<1, \qquad (25b)$$

$$\equiv V_{ap}^* = \text{const}$$

and

$$\dot{m}^* \equiv \frac{\dot{m}}{\rho_a C_c \sqrt{2g}\,(fL_{ap})^{3/2}} = \int_0^{\eta_D} \sqrt{\eta + \frac{\eta_D}{T_n^* - 1} \ln\left[1 - \frac{\eta}{\eta_D}\left(1 - \frac{1}{T_n^*}\right)\right]}\, d\eta$$

$$+ (1 - \eta_D)\sqrt{\eta_D}\sqrt{1 - \frac{\ln T_n^*}{T_n^* - 1}} \qquad (26)$$

Note, that with our specification of the temperature distribution function $T_i(y)$, the dimensionless velocity and rate of mass entrainment depend on just two parameters: T_n^*, the dimensionless corner temperature at the neutral elevation; and η_D, the dimensionless profile development distance (cf. Equations (25) and (26)). Values of $\dot{m}^*$, obtained by integrating Equation (26) numerically, and V_{ap}^* are given in Table I and Figure 3 for a range of values of these parameters. Bounds within which η_D must lie and the means

TABLE I

DIMENSIONLESS RATE OF MASS ENTRAINMENT AND CHARACTERISTIC INFLOW VELOCITY†

η_D		T_n^* 1.02	1.10	1.20	1.30	1.40	1.50
0	$\dot{m}^*$	0	0	0	0	0	0
	V_{ap}^*	0	0	0	0	0	0
.02	$\dot{m}^*$	.0140	.0305	.0419	.0499	.0561	.0612
	V_{ap}^*	.0140	.0306	.0420	.0501	.0564	.0615
.04	$\dot{m}^*$	.0197	.0429	.0589	.0702	.0790	.0862
	V_{ap}^*	.0199	.0433	.0595	.0708	.0797	.0870
.06	$\dot{m}^*$	.0240	.0524	.0719	.0856	.0963	.105
	V_{ap}^*	.0243	.0530	.0728	.0868	.0976	.107
.08	$\dot{m}^*$	.0276	.0602	.0826	.0984	.111	.121
	V_{ap}^*	.0281	.0613	.0841	.100	.113	.123
.10	$\dot{m}^*$	.0307	.0670	.0919	.109	.123	.134
	V_{ap}^*	.0314	.0685	.0940	.112	.126	.138
.12	$\dot{m}^*$	.0335	.0731	.100	.119	.134	.146
	V_{ap}^*	.0344	.0750	.103	.123	.138	.151
.14	$\dot{m}^*$	.0360	.0786	.108	.128	.144	.157
	V_{ap}^*	.0372	.0810	.111	.133	.149	.163
.16	$\dot{m}^*$	.0384	.0836	.115	.137	.154	.168
	V_{ap}^*	.0397	.0866	.119	.142	.159	.174
.18	$\dot{m}^*$	.0405	.0883	.121	.144	.162	.177
	V_{ap}^*	.0421	.0919	.126	.150	.169	.184
.20	$\dot{m}^*$	.0425	.0926	.127	.151	.170	.185
	V_{ap}^*	.0444	.0968	.133	.158	.178	.194

†$\dot{m}^*$ calculated from Equation (26); V_{ap}^* calculated from Equation (25b).

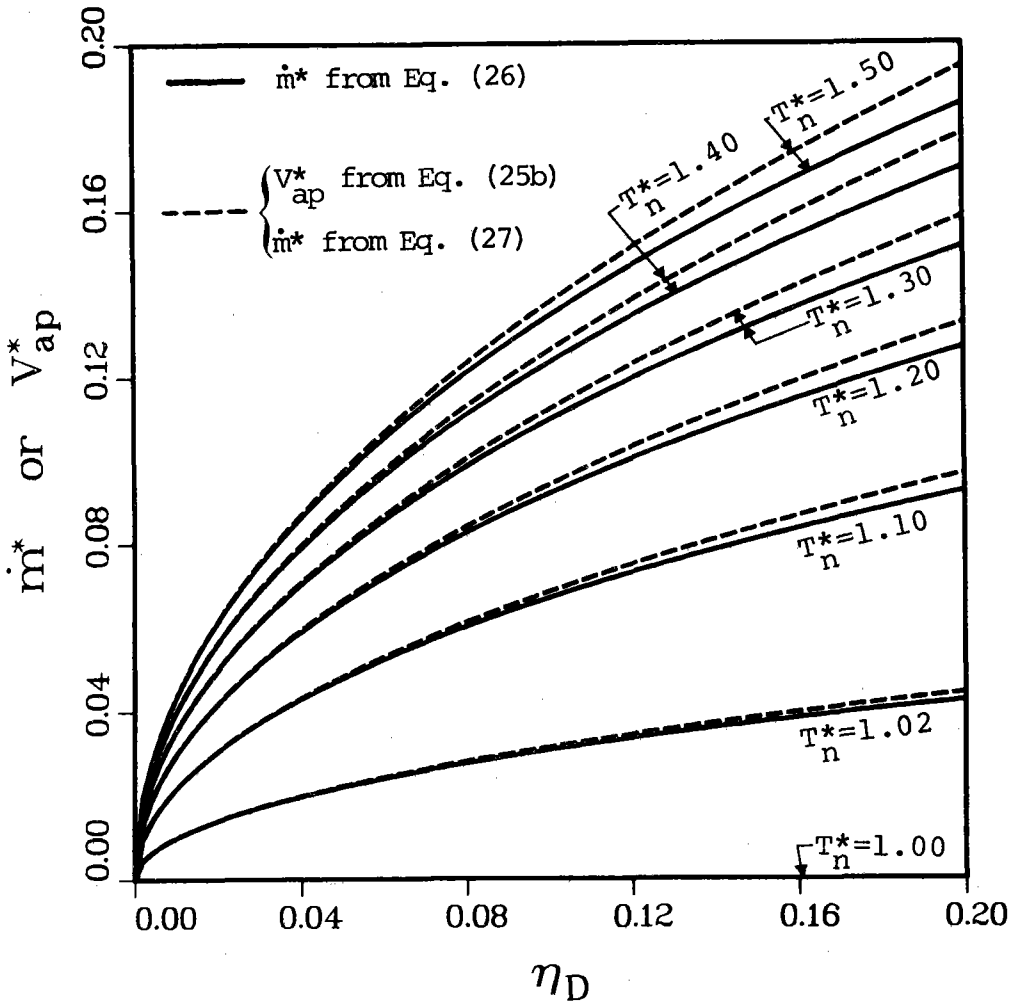

Figure 3. Dimensionless Rate of Mass Entrainment and Aperture Inflow Velocity Versus the Profile Development Parameter η_D

of determining specific values of η_D and T_n^* for a given application are discussed later.

Since available results [3-8] indicate that $\eta_D << 1$, a useful approximation for $\dot{m}^*$ may be obtained simply by neglecting the rate of mass inflow in the velocity development region, by neglecting the integral term and η_D in comparison to unity in Equation (26). This gives

$$\dot{m}^* = \sqrt{\eta_D}\sqrt{1 - \frac{\ln T_n^*}{T_n^* - 1}} \tag{27}$$

The error introduced by using Equation (27) instead of (26) is illustrated in Figure 3, and it is observed that it is small. It is therefore of no consequence that the use of Bernoulli's equation in the velocity development region (where viscous forces are important) may not have been valid. We shall use Equation (27) to express the rate of mass entrainment in the remainder of this study. It is worth noting in addition, that the foregoing expression for $\dot{m}^*$ is identical to the expression for V_{ap}^* (Equation (25b)).

2. Bounds on the Convective Energy Loss and the Rate of Mass Entrainment

An upper bound for the convective loss from a cavity whose interior surfaces are at the temperature T_w is the loss that would occur, hypothetically, if the heat transfer coefficient on all the cavity interior surfaces was that for a vertical free-standing plate of height L_{ap}; i.e.,

$$Q_{max} W_{ap} = h_{fp} A_s (T_w - T_a) \tag{28}$$

where h_{fp} represents the vertical plate heat transfer coefficient, and A_s the cavity surface area. For turbulent natural convection one correlation for h_{fp} is given by [10] as

$$\frac{h_{fp} L_{ap}}{k_f} \equiv Nu_{fp} = 0.13 \left[\frac{g\beta_f (T_w - T_a) L_{ap}^3}{\nu_f^2} Pr_f \right]^{1/3} \tag{29}*$$

*The coefficient 0.13 is not unique: Eckert and Drake [11] use the constant 0.10, Raithby and Hollands [12] use the constant 0.096, etc. Furthermore, in the temperature range of solar receivers, a different constant as well as a variable property parameter may be appropriate.

where the properties are evaluated at the "film" or average temperature $T_f = (T_w+T_a)/2$. The combination of Equations (28) and (29) with the relationships

$$\beta_f = 2/(T_w+T_a) \quad \text{and} \quad Pr_a \approx Pr_f \tag{30}$$

yields the following upper bound for the convective loss

$$Q_{max}\, W_{ap} = \frac{0.26}{Pr_a^{2/3}} \left[\frac{T_w - T_a}{T_w + T_a}\right]^{4/3} \frac{\nu_f^{1/3}}{(2g)^{1/6}}\, \rho_a A_s c_p T_a \sqrt{2g} \tag{31}$$

or simply

$$Q_{max}\, W_{ap} = 0.26\, F \rho_a A_s c_p T_a \sqrt{2g} \tag{32}$$

where

$$F \equiv F(T_w,T_a) = Pr_a^{-2/3} \left(\frac{T_w - T_a}{T_w + T_a}\right)^{4/3} \frac{\nu_f^{1/3}}{(2g)^{1/6}} \tag{33}$$

The function F, which depends only on the cavity and ambient temperatures and the properties of air, proves useful in subsequent calculations and is plotted in Figure 4.

A lower bound for the convective loss from a cavity whose surfaces are at the temperature T_w would be the heat transfer from the hot to cold surfaces of a hypothetical <u>closed</u> box which is geometrically identical to the cavity except for the lack of an aperture. In this enclosure, one vertical surface is assumed to be at the temperature T_w, the surface facing it is assumed to be at the ambient temperature, T_a, and all other surfaces are assumed to be adiabatic. The correlation of MacGregor and Emery [13] is considered to be applicable to such enclosures in turbulent flow and is given by

$$\frac{h_{box} L_{hs}}{k_f} \equiv Nu_{box} = 0.046 \left[\frac{g\beta_f (T_w - T_a) L_{hs}^3}{\nu_f^2} Pr_f\right]^{1/3} \tag{34}*$$

whence the lower bound for the convective loss from a cavity is expressed as

*Here too, the coefficient 0.046 is not unique. Raithby, et al. [14] give a coefficient of 0.044; Jakob's correlation of the data of Mull and Reiher [15] indicates a coefficient of 0.073; etc.

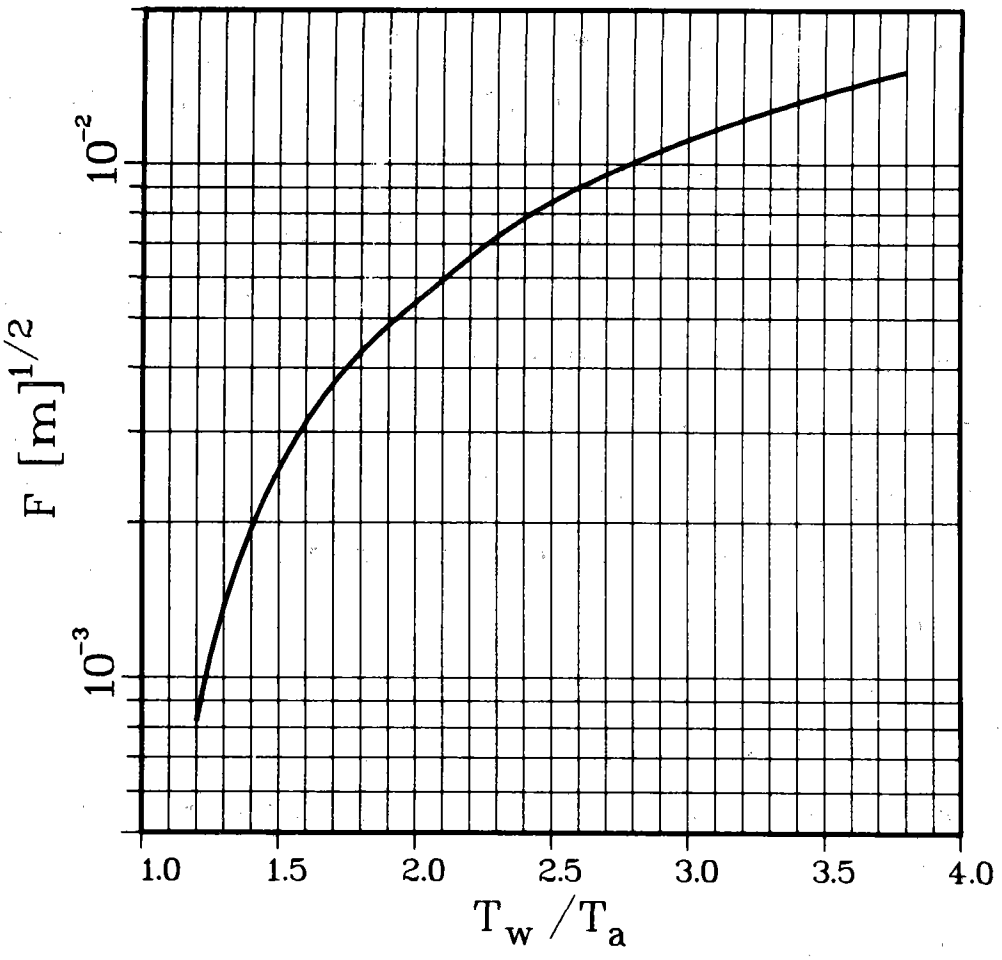

Figure 4. The Property Function F (Equation (33)). Ambient Temperature, T_a, Taken as 293°K. Properties of Air are From [16]

$$Q_{min}\, W_{ap} = h_{box} L_{hs} W_{hs} (T_w - T_a) \tag{35}$$

In these expressions L_{hs} and W_{hs} represent, respectively, the height and width of the heated surface of the hypothetical enclosure. The foregoing lower bound may be more conveniently written as

$$Q_{min}\, W_{ap} = 0.092\, F \rho_a L_{hs} W_{hs} c_p T_a \sqrt{2g} \tag{36}$$

by combining Equations (30), (33-35).

The upper and lower bounds for the convective loss from our 2.15-meter cubic cavity, as calculated by Equations (32) and (36), are plotted in Figure 5. In the calculation of these bounds, five of the cavity walls are considered to be at the temperature T_w, and the sixth is open to the atmosphere which is assumed to be at 293°K. It is clear from their spread that these bounds, by themselves, are not of great utility in obtaining engineering estimates of the convective loss. They do, however, serve as checks for the present and other predictive theories.

Upper and lower bounds on the rate of mass entrainment may be derived from Equation (1), that is

$$\dot{m}_{max\ or\ min} = \frac{Q_{max\ or\ min}}{c_p (T_b - T_a)} \tag{37}$$

where Q_{max} is obtained from Equation (32) or Q_{min} is obtained from Equation (36). The results are

$$\dot{m}_{max} = \frac{0.26\, F \rho_a A_s T_a \sqrt{2g}}{W_{ap} (T_b - T_a)} \tag{38}$$

and

$$\dot{m}_{min} = \frac{0.092\, F \rho_a L_{hs} W_{hs} \sqrt{2g}}{W_{ap} (T_b - T_a)} \tag{39}$$

For a given specification of the bulk temperature, T_b, any flow rate greater than $\dot{m}_{max}$ would correspond to an energy loss greater than Q_{max}; alternatively,

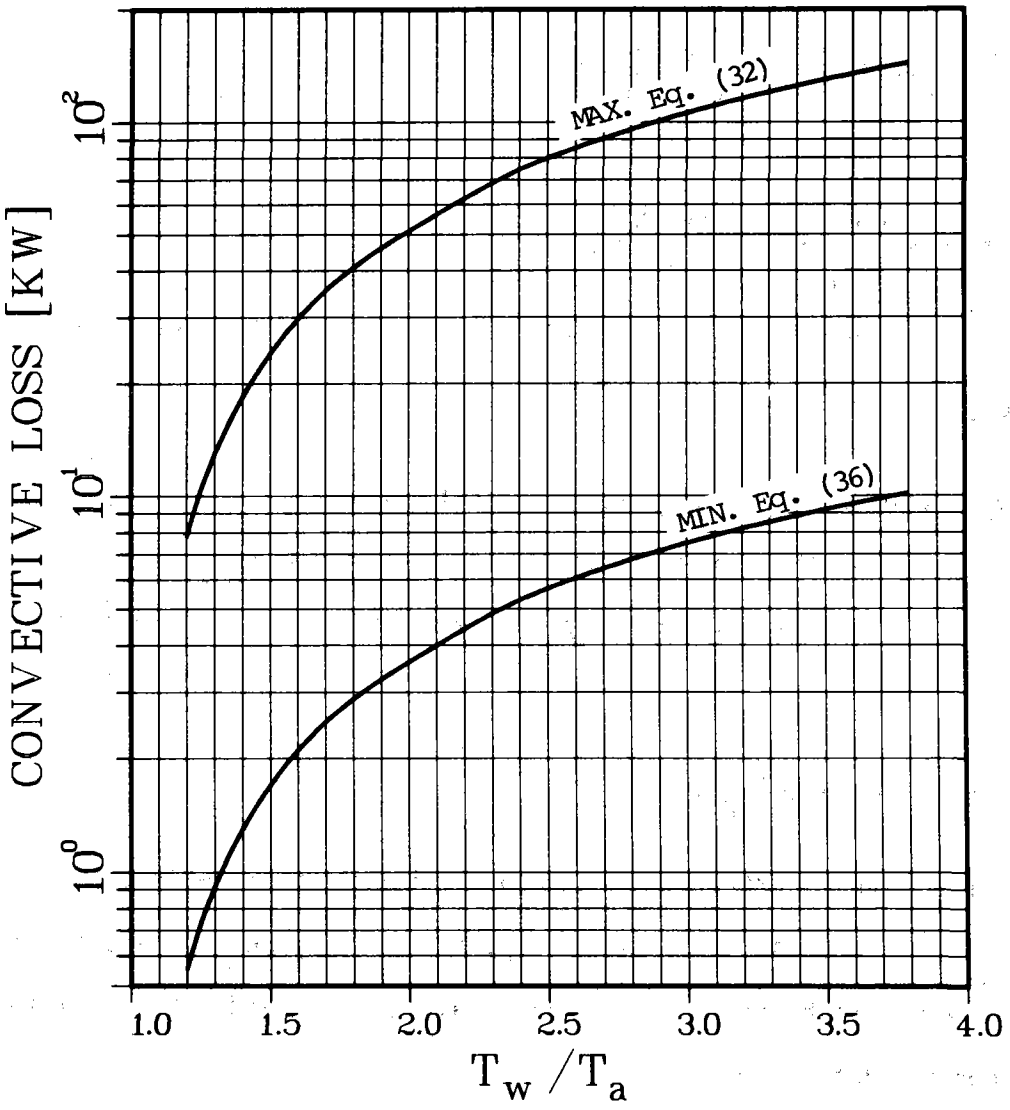

Figure 5. Upper and Lower Bounds on the Convective Loss from the 2.15-meter Cubic Cavity. Five of the Walls are Considered to be at the Uniform Temperature, T_w, and the Sixth (a Vertical Wall) is Open to the Atmosphere. The Atmospheric Temperature, T_a, is Taken to be 293°K

any flow rate less than $\dot{m}_{min}$ would correspond to an energy loss less than Q_{min}. Using the definition of $\dot{m}^*$ (Equation (19)), the corresponding upper and lower bounds on the dimensionless mass entrainment rates are expressed, respectively, as

$$\dot{m}^*_{max} = \frac{0.26\ F}{C_c f^{3/2}(T_b^*-1)} \left(\frac{A_s}{L_{ap}^{3/2} W_{ap}} \right) \tag{40}$$

and

$$\dot{m}^*_{min} = \frac{0.092\ F}{C_c f^{3/2}(T_b^*-1)} \left(\frac{L_{hs} W_{hs}}{L_{ap}^{3/2} W_{ap}} \right) \tag{41}$$

where $T_b^*(=T_b/T_a)$ represents the dimensionless bulk temperature of the heated emerging air.

3. The Bulk Temperature of the Heated Emerging Air

The bulk temperature of the emerging air, T_b, is defined such that the product $\dot{m}c_pT_b$ represents the enthalpy efflux from the cavity aperture, i.e.,

$$\dot{m}c_pT_b \equiv \int_0^{\xi_n} \rho(\xi)u(\xi)c_p\ T(\xi)d\xi \tag{42}$$

where ξ_n denotes the aperture height occupied by the outflow (cf. Figure 2a) and $\rho(\xi)$ and $T(\xi)$ represent, respectively, the density and temperature distributions over this height. Using the ideal gas law, and with the rate of mass entrainment defined by

$$\dot{m} = \int_0^{\xi_n} \rho(\xi)u(\xi)d\xi\ , \tag{43}$$

the bulk temperature may, in turn, be expressed as

$$T_b = \frac{\int_0^1 u(\lambda)d\lambda}{\int_0^1 [u(\lambda)/T(\lambda)]d\lambda} \tag{44}$$

where λ is the dummy variable, ξ/ξ_n. The pressure and the specific heat have been assumed to be constants.

It is seen that a priori knowledge of the velocity and temperature distributions is necessary to calculate the bulk temperature. Since these distributions are generally unknown, we have assumed distributions that are in qualitative agreement with the results of Penot [5], and Humphrey, et al. [7]. They are:

$$u(\lambda) = U \frac{\lambda(1-\lambda)e^{a\lambda}}{\lambda_m(1-\lambda_m)e^{a\lambda_m}} \tag{45}$$

where

$$a = (2\lambda_m-1)/[\lambda_m(1-\lambda_m)] \tag{46}$$

and

$$T(\lambda) = T_a \Bigg/ \left[1 - \lambda\left(1 - \frac{T_a}{T_w}\right)\right]. \tag{47}$$

U represents the maximum velocity of the emerging air, and λ_m the dimensionless location of this maximum above the neutral elevation. These distributions are plotted in Figure 6a and it should be noted that they satisfy the physical requirements that u=0 at λ=0 and λ=1; and T=T_w at λ=1. Equation (47) also implies that T=T_a at λ=0, a condition which, if not strictly valid, has little effect upon the computation of the bulk temperature since $u(\lambda)\to 0$ as $\lambda\to 0$ (cf. Equation (44)). The expression for the bulk temperature, obtained by substituting Equations (45) and (47) into (44), is

$$T_b/T_a \equiv T_b^* = \frac{a[a(1+e^a) + 2(1-e^a)]}{a^2(1+e^a/T_w^*)+2a[e^a-1/T_w^*-2(e^a/T_w^*-1)]+6(1-1/T_w^*)(1-e^a)} \tag{48}$$

where T_w^* denotes the dimensionless wall temperature, T_w/T_a. Equation (48) is plotted in Figure 7 for values of a corresponding to λ_m = .7, .8, and .9.

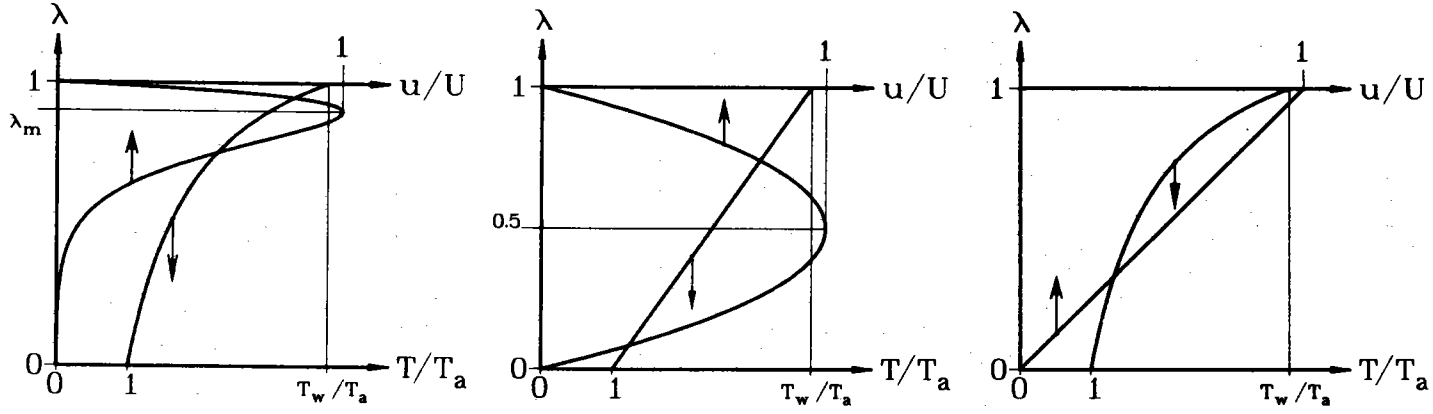

$$\frac{u(\lambda)}{U} = \frac{\lambda(1-\lambda)e^{a\lambda}}{\lambda_m(1-\lambda_m)e^{a\lambda_m}}$$

$$\frac{T(\lambda)}{T_a} = \frac{1}{1-\lambda\left(1-\frac{T_a}{T_w}\right)}$$

(a)

$$\frac{u(\lambda)}{U} = 4\lambda(1-\lambda)$$

$$\frac{T(\lambda)}{T_a} = 1 + \lambda\left(\frac{T_w}{T_a} - 1\right)$$

(b)

$$\frac{u(\lambda)}{U} = \lambda$$

$$\frac{T(\lambda)}{T_a} = \frac{1}{1-\lambda\left(1-\frac{T_a}{T_w}\right)}$$

(c)

Figure 6. Velocity and Temperature Distributions in Heated Emerging Air
(a) Recommended Distributions
(b) and (c) Other Distributions That Have Been Considered

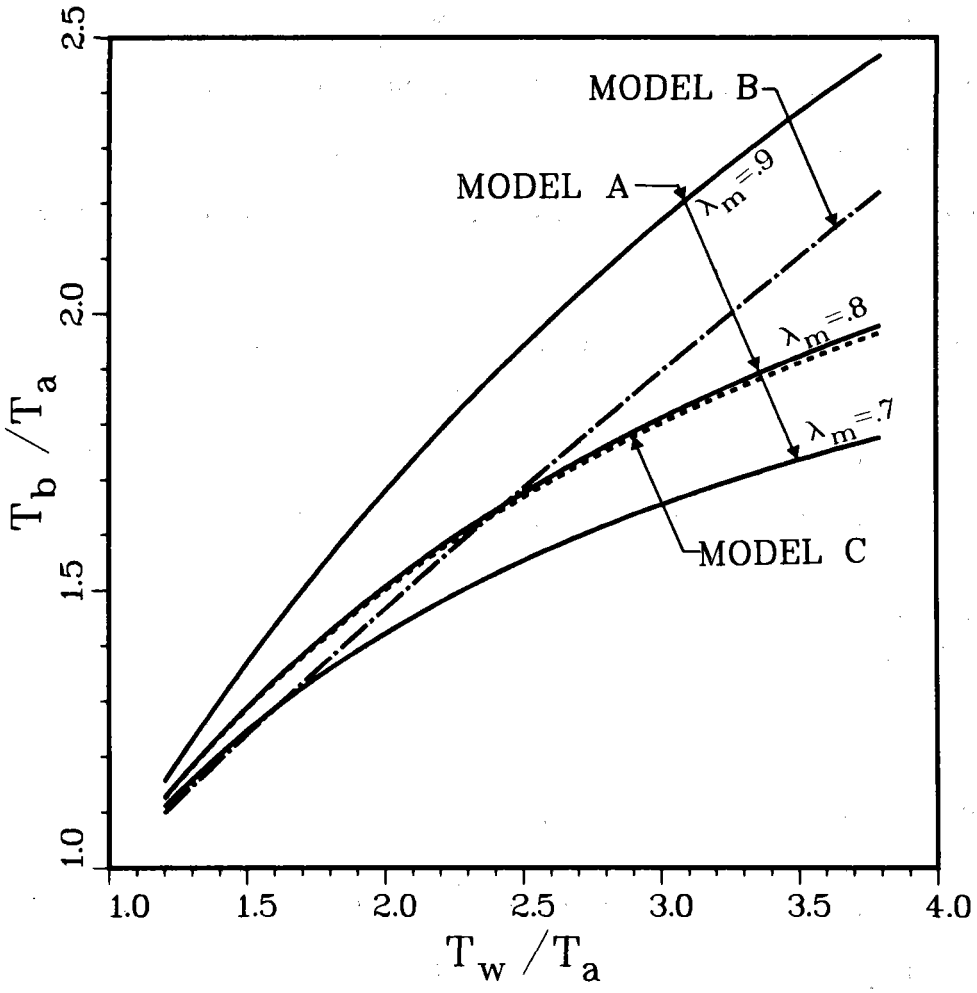

Figure 7. The Bulk Temperature of the Heated Emerging Air for Various Distributions of the Velocity and Temperature
Model A Corresponds to Figure 6a
Model B Corresponds to Figure 6b
Model C Corresponds to Figure 6c

We have also considered other forms of the velocity and temperature distributions, and these are depicted in Figures 6b and 6c. The corresponding expressions for the bulk temperature have been determined and the results are plotted in Figure 7. Equation (48) (Model A) is, however, recommended and is used in the remainder of this study.

4. An Alternative Formulation for the Convective Loss

Having expressions for the rate of mass entrainment and the bulk temperature, it is possible to calculate the convective loss directly from Equation (1) upon specifying certain parameters. It is found convenient, however, to use an alternative formulation.

By expressing the convective loss as

$$Q = Q_{max} \left(\frac{Q}{Q_{max}} \right) , \tag{49}$$

and then substituting Q_{max} from Equation (32) and the result

$$\frac{Q}{Q_{max}} = \frac{\dot{m}^*}{\dot{m}^*_{max}} \tag{50}$$

we obtain

$$QW_{ap} = 0.26 \sqrt{2g}\, F \rho_a A_s c_p T_a \left(\frac{\dot{m}^*}{\dot{m}^*_{max}} \right) \tag{51}$$

Equation (50) arises from the combination of Equations (1), (37) and from the definition of $\dot{m}^*$ (Equation (26)). From Equation (27),

$$\frac{\dot{m}^*}{\dot{m}^*_{max}} = \sqrt{\frac{\eta_D}{\eta_{D,max}}} \tag{52}$$

whence Equation (51) becomes

$$\boxed{QW_{ap} = 0.26 \sqrt{2g}\, F \rho_a A_s c_p T_a \sqrt{\frac{\eta_D}{\eta_{D,max}}}} \tag{53}$$

The quantity $\eta_{D,max}$ is defined such that (cf Eq. (27)):

$$\dot{m}^*_{max} \equiv \sqrt{\eta_{D,max}} \sqrt{1 - \frac{\ln T_n^*}{T_n^* - 1}} \tag{54}$$

Physically, it represents an upper bound on the profile development parameter since any value of η_D greater than $\eta_{D,max}$ corresponds to a convective energy loss greater than Q_{max}. Combining Equations (40) and (54) yields

$$\eta_{D,max} = \left[\frac{0.26\ F}{C_c f^{3/2}(T_b^* - 1)}\left(\frac{A_s}{L_{ap}^{3/2} W_{ap}}\right)\right]^2 \frac{1}{1 - \frac{\ln T_n^*}{T_n^* - 1}} \tag{55}$$

Equation (53) is the alternative formulation sought. Its advantage is that all of the parameters requiring ad hoc specification are embodied in the ratio $\eta_D/\eta_{D,max}$. It can be verified that Equation (53) is identical to the result that would be obtained by substituting the expressions for $\dot{m}$ and T_b directly into Equation (1).

The convective loss from our 2.15-meter cavity as calculated by Equation (53) is plotted in Figure 8 as a function of the wall temperature ratio for various values of the ratio $\eta_D/\eta_{D,max}$.

Summary and Conclusions

We present a simple theory for predicting the convective energy loss and mass entrainment rate for side-facing cavity-type receivers in windless environments. The convective loss is expressed by Equation (53), and the mass entrainment rate by Equation (27). Although, at present, the lack of experimental measurements makes it impossible to test the accuracy of this theory, it should be noted that similar theoretical approaches in the building sciences have been successful.

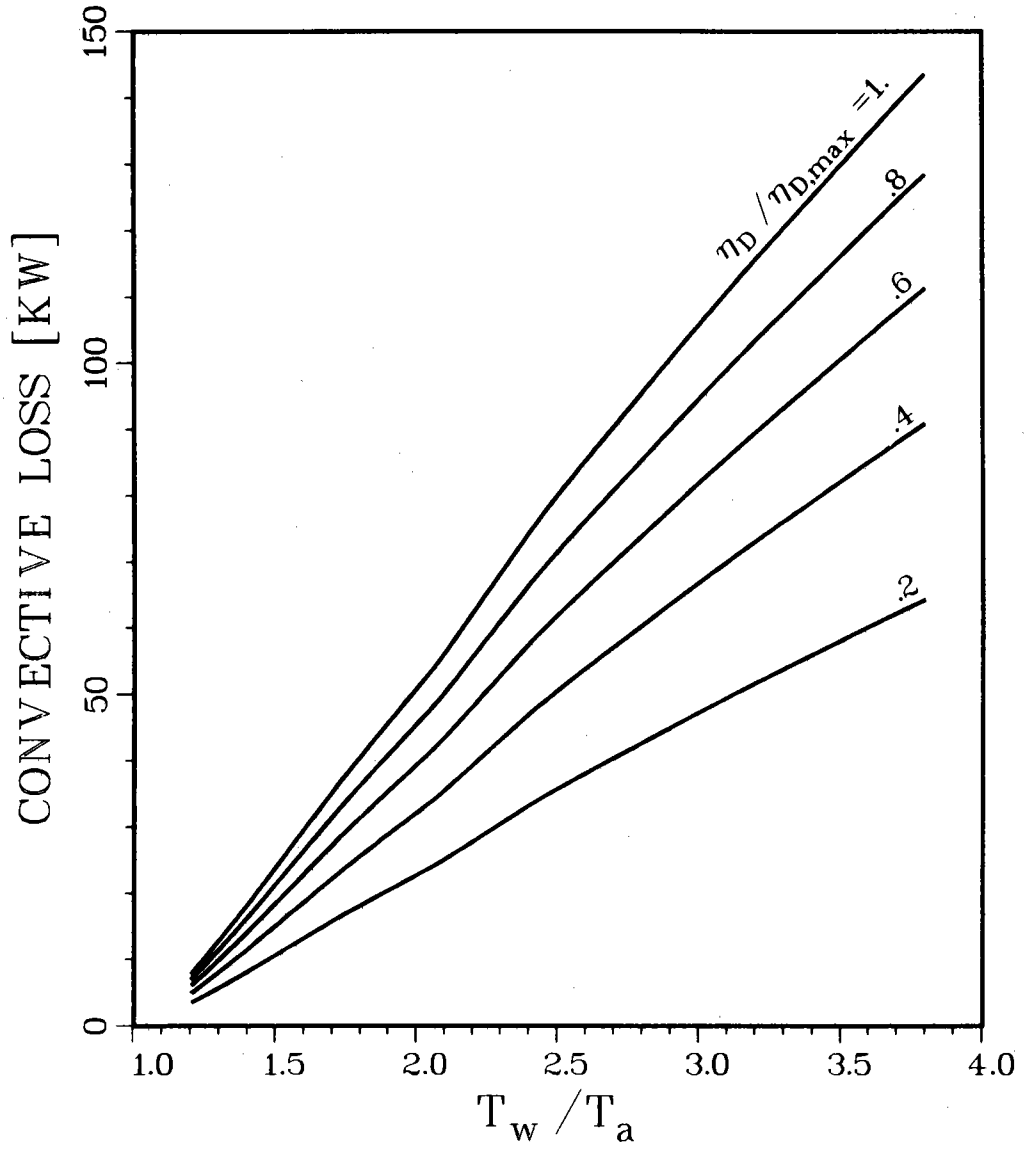

Figure 8. Convective Loss from 2.15-meter Cubic Cavity Computed with Equation (53). Ambient Temperature, T_a, Taken to be 293°K

The chief drawback in implementing the theory is the need to specify a number of parameters, some of which are only tenuously known. These parameters are

f, the fraction of the aperture height occupied by the inflow;

C_c, the contraction coefficient;

λ_m, the dimensionless location of the velocity maximum above the neutral elevation (cf. Figure 6a);

T_n^*, the dimensionless temperature of the stagnant air alongside the vena contracta at the neutral elevation; and

η_D, the dimensionless profile development distance for incoming air, y_D/y_n (cf. Figure 2c).

Our recommendations for the specifications of these parameters and a sample calculation are given in the Appendix.

A number of assumptions have been made in arriving at the final formalisms. The one that we regard as being crucial, however, is the presumption that the incoming velocity distribution is shaped, qualitatively, as depicted in Figure 2a.

The theory as presented here is strictly applicable to cavities whose apertures are rectangular and vertical. We judge it feasible to relax these restrictions within the framework of the building sciences approach.

The greatest need in our view is the acquisition of experimental data to test the accuracy of this predictive theory. This need should be satisfied shortly with results from our 2.15 meter cubic cavity.

APPENDIX--ESTIMATION OF VALUES OF PARAMETERS NEEDED FOR COMPUTATIONS AND A SAMPLE CALCULATION

We present here our recommendations for the specification of the parameters needed to calculate the convective loss. Modifications of these recommendations may be necessary as experimental and numerical data become available.

f--The measurements of Shaw [2], Quintiere and DenBraven [3], and Steckler et al. [8] indicate values of f that vary from 0.48 to 0.68. We recommend, tentatively, the approximate mid-point of this range, i.e., f = 0.55.

C_c--Following Streeter [9], we assume $C_c = 0.6$. This value corresponds to the flow from an infinite reservoir through a finite opening. It also correlates some of the data of Brown and Solvason [1] and Shaw [2]. We point out, however, that the recent data of Steckler et al. [8] indicate a value of 0.7.

λ_m--An examination of the available experimental and numerical data has revealed values of λ_m between ~ 0.5 (Shaw [2]) and ~ 0.9 (Humphrey, et al. [7]). The midpoint of this range, $\lambda_m = 0.7$, is tentatively recommended.

T_n^*--Information on T_n^* must strictly come from three-dimensional numerical or experimental studies. Since no pertinent studies have been reported, our specification of T_n^* is based on the fact that its role in the present theory is to fix the density of air in the stagnant column alongside the vena contracta. Accordingly we assume that

$$\rho_n = \frac{1}{2} (\rho_w + \rho_a) \ . \qquad (A.1)$$

Using the ideal gas law and the definition of the dimensionless temperature this leads to

$$T_n^* = \frac{2}{\frac{1}{T_w^*} + 1} \tag{A.2}$$

η_D--Suitable numerical or experimental data for this parameter are also lacking, and therefore, our specification of $\eta_D (\equiv y_D/y_n)$ is based on a model which describes the development of the boundary layer between the neutral surface and the incoming air stream. In this model it is assumed that the incoming air stream accelerates toward the cavity aperture according to the relationship

$$V(x) = v_1 x^m \tag{A.3}$$

where x denotes the distance measured toward the cavity from the origin of the inflow; V(x) represents the free stream velocity outside the boundary layer; and v_1 and m are constants. (Note that $V(x) = V_{ap}$ at x corresponding to the aperture plane.) The development of such a boundary layer is described by the Falkner-Skan equation (Schlichting [17, p. 150]) if the inflow in the neighborhood of the neutral surface is laminar, and if no flow crosses the neutral surface. This model leads to the result that

$$\eta_D = 0.011\, L_{ap}^{-3/5} \left[1 - \frac{\ln T_n^*}{T_n^* - 1}\right]^{-1/5} \tag{A.4}$$

by assuming that the exponent m=4 in Equation (A.3); and the virtual origin of the inflow is located at $0.3\, L_{ap}$ meters outside the cavity aperture.

It should be noted that, having already specified the parameters f, C_c, λ_m, and T_n^*, the selection of η_D is governed by the requirement that

$$\eta_{D,max} > \eta_D > \eta_{D,min} .$$

$\eta_{D,max}$ is given by Equation (55) which is repeated here for convenience:

$$\eta_{D,max} = \left[\frac{0.26\ F}{C_c f^{3/2}(T_b^*-1)}\left(\frac{A_s}{L_{ap}^{3/2}W_{ap}}\right)\right]^2 \frac{1}{1 - \frac{\ln T_n^*}{T_n^*-1}} \quad ; \tag{55}$$

and $\eta_{D,min}$ is a lower bound defined such that

$$\dot{m}^*_{min} \equiv \sqrt{\eta_{D,min}}\sqrt{1 - \frac{\ln T_n^*}{T_n^*-1}} \tag{A.5}$$

(cf. Equation (27)). By combining Equation (A.5) with the expression for $\dot{m}^*_{min}$ (Equation (41)), we have that

$$\eta_{D,min} = \left[\frac{0.092\ F}{C_c f^{3/2}(T_b^*-1)}\left(\frac{L_{hs}W_{hs}}{L_{ap}^{3/2}W_{ap}}\right)\right]^2 \frac{1}{1 - \frac{\ln T_n^*}{T_n^*-1}} \tag{A.6}$$

To aid in the computations of $\eta_{D,max}$ and $\eta_{D,min}$ for the current specification of the parameters, we have plotted in Figure A.1 the function

$$G \equiv \left[\frac{F}{C_c f^{3/2}(T_b^*-1)}\right]^2 \frac{1}{1 - \frac{\ln T_n^*}{T_n^*-1}} \tag{A.7}$$

versus the temperature ratio T_w/T_a. With a numerical value for G, $\eta_{D,max}$ and $\eta_{D,min}$ can be readily determined from the relationships:

$$\frac{\eta_{D,max}}{\left[.26\left(\frac{A_s}{L_{ap}^{3/2}W_{ap}}\right)\right]^2} = \frac{\eta_{D,min}}{\left[.092\left(\frac{L_{hs}W_{hs}}{L_{ap}^{3/2}W_{ap}}\right)\right]^2} = G \tag{A.8}$$

We shall now calculate the convective loss, mass entrainment rate and characteristic inflow velocity for our 2.15-meter cubic cavity in order to illustrate the use of this theory. Equation (53) will be employed for the convective loss. For concreteness, we presume the temperature of the cavity surfaces to be uniform and at 800°K.

Figure 4 gives $F = 9.71 \times 10^{-3}\ m^{1/2}$ and Figure A.1 gives $G = 2.44 \times 10^{-2}$ m. The geometrical parameter $[A_s/(L_{ap}^{3/2}W_{ap})] = 3.41\ m^{-1/2}$ whence $\eta_{D,max} = 0.019$ using Equation (A.8).

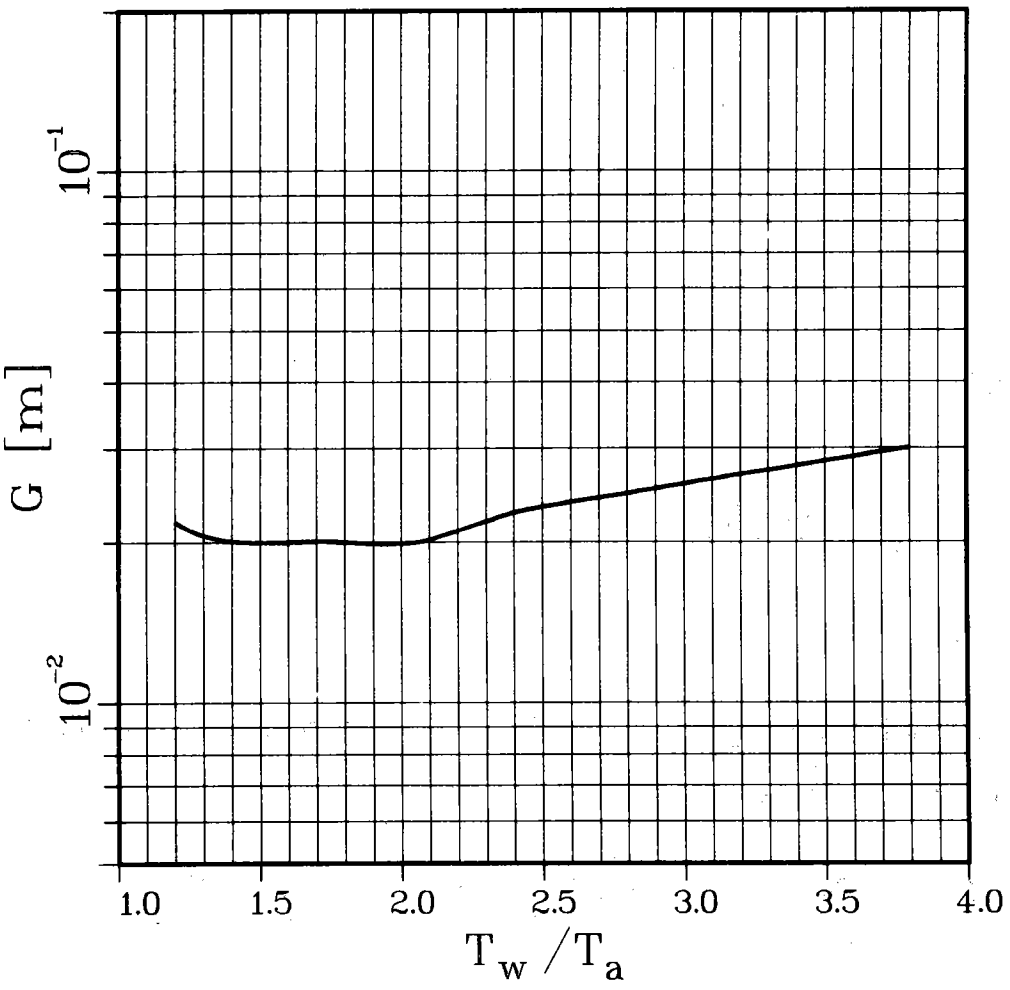

Figure A.1. The Function G (Equation (A.7)). Assumes $C_c = 0.6$, $f = 0.55$, $\lambda_m = 0.7$ and T_n^* Given by Equation (A.2)

The substitution of the foregoing numerical values and $\eta_D = 0.010$ (from Equation (A.4)) into Equation (53) thus gives:

$$QW_{ap} = 0.26 \sqrt{2 \times 9.81 \frac{m}{sec^2}} \times 9.71 \times 10^{-3} \, m^{1/2} \times$$

$$1.21 \frac{kg}{m^3} \times 5 \times 2.15^2 \, m^2 \times$$

$$1.00 \frac{kw\text{-}sec}{Kg\text{-}°K} \times 293°K \times$$

$$\sqrt{\frac{.010}{.019}}$$

$$= 66 \text{ kw}$$

The <u>dimensionless</u> rate of mass entrainment as expressed by Equation (27) has the value

$$\dot{m}^* = \sqrt{0.010} \sqrt{1 - \frac{\ln 1.46}{.46}}$$

$$= 0.042$$

and the corresponding <u>dimensional</u> rate of mass entrainment using the definition in Equation (26) is found to be

$$\dot{m} = 0.042 \left[1.21 \frac{kg}{m^3} \times .6 \times \sqrt{2 \times 9.81 \frac{m}{sec^2}} \times (.55 \times 2.15 \text{ m})^{3/2} \right]$$

$$= 0.17 \frac{kg}{m\text{-}sec}$$

In these calculations, T_n^* is given by Equation (A.2). The characteristic inflow velocity, determined from Equation (25b), has the value

$$V_{ap} = 0.042 \left[.6 \times \sqrt{2 \times 9.81 \frac{m}{sec^2}} \times \sqrt{.55 \times 2.15 \text{ m}} \right] = 0.12 \frac{m}{sec}$$

The sensitivity of the foregoing calculation to the specification of the parameters has been assessed by increasing and then decreasing the parameters f, C_c, λ_m, and T_n^* by 10% from their nominal values. The resultant calculated values of the convective energy loss are, respectively, 92 and 42 kw. As implied earlier, there are presently no data to judge the reasonableness of these limits.

REFERENCES

1. W. G. Brown and K. R. Solvason, "Natural Convection Through Rectangular Openings in Partitions - 1", Int. J. Heat Mass Transfer, 5, pp. 859-868, 1962.

2. B. H. Shaw, "Heat and Mass Transfer by Natural Convection and Combined Natural Convection and Forced Air Flow Through Large Rectangular Openings in a Vertical Partition," Symposium on Heat and Mass Transfer by Combined Forced and Natural Convection, Institution of Mechanical Engineers, London, 15 September 1971.

3. J. G. Quintiere and K. DenBraven, "Some Theoretical Aspects of Fire Induced Flows Through Doorways in a Room-Corridor Scale Model," National Bureau of Standards Report NBSIR 78-1512, National Bureau of Standards, Washington, D.C., October 1978.

4. F. Penot, "Transfert de chaleur par convection naturelle dans une cavite rectangulaire isotherme ouverte sur une face," Revue Phys. Appl., 15, pp. 207-212, 1980.

5.* F. Penot, Private Communication, January 1980.

6. L. L. Eyler, "Predictions of Convective Losses from a Solar Cavity Receiver," ASME Paper 80-C2/Sol-8, August 1980.

7. J. A. C. Humphrey, et al., "Investigation of Free-Forced Convection Flows in Cavity-Type Receivers," Mid-Term Report for Sandia Laboratories under Contract P.R. 20-1012, July 1980.

8. K. D. Steckler, et al., "Fire Induced Flows through Room Openings - Flow Coefficients," Presented at the Eastern States Combustion Institute Meeting, November 1980.

9. V. L. Streeter, Editor, "Handbook of Fluid Dynamics", p. 3-21, McGraw-Hill Book Co., Inc., New York, 1961.

10. W. H. McAdams, "Heat Transmission," Third Edition, McGraw-Hill Book Co., Inc., New York, 1954.

11. E. R. G. Eckert and R. M. Drake, Jr., "Heat and Mass Transfer", Second Edition, McGraw-Hill Book Co., New York, 1959.

*This reference contains details of velocity distributions which did not appear in Reference 4.

12. G. D. Raithby and K. G. T. Hollands, "Laminar and Turbulent Free Convection From Elliptic Cylinders, with a Vertical Plate and Horizontal Circular Cylinder as Special Cases," Trans. ASME, J. of Heat Transfer, Vol. 98, pp. 72-80, 1976.

13. R. K. MacGregor and A. F. Emery, "Free Convection Through Vertical Plane Layers--Moderate and High Prandtl Number Fluids," Trans. ASME, J. of Heat Transfer, Vol. 91, pp. 391-403, 1969.

14. G. D. Raithby, K. G. T. Hollands and T. E. Unny, "Analysis of Heat Transfer by Natural Convection Across Vertical Fluid Layers," Trans. ASME, J. of Heat Transfer, Vol. 99, pp. 287-293, 1977.

15. M. Jakob, "Heat Transfer", Vol. I, John Wiley and Sons, Inc., New York, 1958.

16. J. Hilsenrath, et al., "Tables of Thermodynamic and Transport Properties of Air, A, CO_2, CO, H_2, N_2, O_2, and Steam", NBS Circular 564, 1960.

17. H. Schlichting, "Boundary-Layer Theory", Sixth Edition, McGraw-Hill Book Co., Inc., New York, 1968.

INITIAL DISTRIBUTION

U.S. Department of Energy
Washington, D.C. 20545
Attn: J. E. Rannels
M. U. Gutstein
G. W. Braun

Division of Solar Technology
U.S. Department of Energy
San Francisco Operations Office
1333 Broadway
Oakland, CA 94612
Attn: S. D. Elliot
R. W. Hughey

Solar Energy Research Institute
1536 Cole Boulevard
Golden, CO 80401
Attn: F. Kreith
B. P. Gupta
J. Lefferdo

Aerospace Corporation
P. O. Box 92957
Los Angeles, CA 90009
Attn: P. Mathur
P. Derienzo

Professor R. Greif
College of Engineering
Department of Mechanical Engineering
University of California, Berkeley
Berkeley, CA 94720

Professor R. Viskanta
School of Mechanical Engineering
Purdue University
West Lafayette, Indiana 47907

Professor Milton B. Larson
Department of Mechanical Engineering
Rogers Hall
Oregon State University
Corvallis, Oregon 97331

Professor E. Somerscales
Rensselaer Polytechnic Institute
College of Engineering
Troy, NY 12181

Professor J. A. C. Humphrey
College of Engineering
Department of Mechanical Engineering
University of California, Berkeley
Berkeley, CA 94720

Dr. L. L. Eyler
Battelle Pacific Northwest Laboratories
P. O. Box 999
Richland, Washington 99352

Professor V. Sernas
Rutgers State University of New Jersey
College of Engineering
P. O. Box 909
Piscataway, NJ 08854

SRI International
333 Ravenswood Avenue
Menlo Park, CA 94025
Attn: A. J. Slemmons

Dr. P. Le Quere
Laboratoire D' Energetique Solaire
40 Avenue du Rector Pineau
86022 Poitiers
France

Professor F. S. Sherman
College of Engineering
Department of Mechanical Engineering
University of California, Berkeley
Berkeley, CA 94720

D. B. Hayes, 5510; Attn: J. W. Nunziatio, 5511
D. F. McVey, 5512
D. W. Larson, 5513
J. H. Scott, 4700; Attn: G. E. Brandvold, 4710
V. L. Dugan, 4720; Attn: W. P. Schimmel, Jr., 4723
T. B. Cook, 8000; Attn: W. J. Spencer, 8100
A. N. Blackwell, 8200
B. F. Murphey, 8300
W. E. Alzheimer, 8120; Attn: G. A. Benedetti, 8121
C. S. Hoyle, 8122
W. D. Zinke, 8123
R. J. Gallagher, 8124
M. Abrams, 8124 (25)
J. S. Kraabel, 8124
L. Gutierrez, 8400; Attn: C. S. Selvage, 8420
R. C. Wayne, 8450; Attn: P. J. Eicker, 8451
A. C. Skinrood, 8452
A. F. Baker, 8452 (5)
C. E. Hackett, 8452
W. G. Wilson, 8453 (40)
E. T. Cull, Jr., 8453

Publications Division, 8265, for TIC (2)
Library and Security Classification Division, 8266 (5)
Technical Library Processes and Systems Division, 3141 (4)
Education Division, 8214 (3)

Org.	Bldg.	Name	Rec'd by *	Org.	Bldg.	Name	Rec'd by *

* Recipient must initial on classified documents.